Journal of Alloys and Compounds 950 (2023) 169883

Contents lists available at ScienceDirect

Journal of Alloys and Compounds

journal homepage: www.elsevier.com/locate/jalcom

First-order phase transition in high-performance La(Fe,Mn,Si)$_{13}$H despite negligible hysteresis

Luis M. Moreno-Ramírez [a], Jia Yan Law [a], Josefa M. Borrego [a], Alexander Barcza [b], Jean-Marc Greneche [c], Victorino Franco [a,*]

[a] Department of Condensed Matter Physics, ICMS-CSIC, University of Seville, P.O. Box 1065, 41080 Seville, Spain
[b] Vacuumschmelze GmbH & Co. KG, Gruener Weg 37, 63450 Hanau, Germany
[c] Institut des Molécules et Matériaux du Mans, UMR CNRS 6283, IMMM, Le Mans Université, 72085 Le Mans, France

ARTICLE INFO

Article history:
Received 11 February 2023
Received in revised form 5 March 2023
Accepted 28 March 2023
Available online 29 March 2023

Keywords:
Magnetocaloric effect
First-order phase transitions
Exponent *n* criteria
High-performance La(Fe,Mn,Si)$_{13}$H
Low hysteresis

ABSTRACT

Optimizing the performance of magnetocaloric materials is facilitated by understanding the thermomagnetic transitions they undergo, including the order of these transitions and their strength. Those exhibiting strong first-order phase transitions (FOPT) are accompanied by large heating and cooling responses but with relatively small cyclic responses, while materials with second-order (SOPT) character exhibit moderate heating and cooling responses. However, the lack of hysteresis could partially compensate for the lower magnitudes with a more cyclic response. One way to effectively maximize the cyclic response, combining the advantages of FOPT and SOPT, is to fine tune the transition towards the borderline of FOPT-SOPT, which can minimize hysteresis. For the well-known La(Fe,Si)$_{13}$ family, it is challenging to identify and/or evaluate the critical point where FOPT crossovers to SOPT based on conventional techniques. To address these ambiguities, in this work, we apply the field dependence exponent *n* criteria to a series of lowly hysteretic and high-performance La(Fe,Mn,Si)$_{13}$H magnetocaloric materials with compositions close to the critical one. Even if the sample with the lowest hysteresis resembles characteristics of SOPT, it is evidently identified as undergoing FOPT from the *n* criteria: (1) existence of $n > 2$ overshoot and (2) *n* at the transition temperature, $n_{transition}$, is 0.37. This proximity to the critical composition ($n_{transition}$=0.4) further explains the low hysteresis observed. This FOPT character of the series is confirmed by temperature-dependent ^{57}Fe Mössbauer spectrometry studies, fitting the hyperfine field to the Bean-Rodbell model instead of the usual Brillouin function. As it is a zero-field method, the confirmation by Mössbauer spectrometry gives further strength to the *n*-criterion.

1. Introduction

Over 20% of the total electricity consumption landscape accounts for temperature control applications and the trend is expected to grow further as global warming and financial development of equatorial countries continue (which population will have a larger demand of refrigeration systems) [1–3]. Domestic refrigerators have been based on the expansion/compression of gases since the early development of the technology. However, despite their ability to cover desired temperature control ranges, these systems are energy inefficient (due to the compressor) and use hazardous or contaminating chemicals (such as chlorofluorocarbons, liquefied ammonia or hydrochlorofluorocarbons). There has been research on the possibility of magnetocaloric refrigeration devices that will solve the mentioned problems of conventional systems, such as larger energy efficiency and the use of green materials [4–9]. They are based on the magnetocaloric effect (MCE), which involves reversible changes in temperature/entropy of magnetic materials subjected to magnetic field variation in adiabatic/isothermal conditions, with the relevant magnitudes being the adiabatic temperature change (ΔT_{ad}) and the isothermal entropy change (ΔS_{iso}). To maximize the effect, the magnetization must be strongly temperature/field dependent; consequently, the magnetocaloric effect is directly related to the study of thermomagnetic phase transitions [10].

First-order thermomagnetic transitions (FOPT) in magnetocaloric materials typically lead to obtaining giant MCE [11–16]. Although a giant response is highly desirable, the reversibility in the magnetocaloric response is reduced because the nature of FOPT involves thermal hysteresis [17,18]. This undesirable hysteresis severely reduces the response of the material under working conditions. The straight-forward

* Corresponding author.
E-mail address: vfranco@us.es (V. Franco).

https://doi.org/10.1016/j.jallcom.2023.169883

solution to avoid hysteresis is to change from FOPT to second-order phase transition (SOPT). However, this is usually at the expense of a largely compensated magnetocaloric response. Despite this, thermal hysteresis can be reduced by magnetic field, so it is not necessary to completely change the order of the transition from FOPT to SOPT but approaching the critical composition where FOPT crossovers to SOPT. In other words, regardless of the magnetic field change, the closer the SOPT materials are to the critical point, the better their magnetocaloric responses will be. Conversely, the optimization of FOPT materials is more complicated since it relies on the magnetic field change, which can partially overcome the thermal hysteresis. For moderate magnetic field changes of 1–2 T, the typical range employed in real devices, magnetocaloric materials with moderate FOPT character are optimal, i.e., close to the critical composition but keeping the first-order character [19–21]. It is therefore crucial to determine the critical composition to develop new materials with optimized performance. However, materials near the borderline of both transitions can be difficult to label as FOPT or SOPT, which can affect the optimization process.

For the identification of the order of phase transitions undergone by magnetocaloric materials, the common methods used by the community are [10,22]: the shapes of the MCE curves (FOPT: abrupt; SOPT: gradual/smeared out shape), existence of hysteresis, the collapse on universal curve (SOPT: perfect collapse on single curve; FOPT: no collapse of the rescaled curves), Banerjee´s criterion (FOPT: negative slope; SOPT: positive slope) or calorimetric ones (FOPT: singularity; SOPT: discontinuity in the heat capacity). All of these methods are affected by subjective interpretation of the data analysis, except for the Banerjee´s criterion, which is a quantitative criterion. However, it shows discrepancies with other methods as it can be significantly affected by the presence of magnetic impurities or if the materials cannot be described by mean field theories [20,23,24]. Recently, the field dependence exponent n has been found addressing the limitations of these conventional techniques to determine the order of phase transitions and the critical composition [22,25]. The identification of FOPT is clearly indicated by the criterion of overshoot of $n > 2$ near the transition temperature, while the absence of this overshoot indicates for SOPT. Moreover, $n = 0.4$ at the transition temperature for zero field distinctly distinguishes the critical point when transforming from FOPT to SOPT, $n < 0.4$ indicates FOPT and $n > 0.4$ indicates SOPT [25]. As a result, using the value of n, we can distinguish not only the order of the transformation, but also its strength (moderate/strong FOPT) depending on the proximity to the critical composition.

In this work, we have further applied this exponent n criterion to a series of high-performance and weakly hysteretic (therefore, challenging to evaluate for the order of phase transition) $La(Fe,Mn,Si)_{13}H$ compounds in order to shed more light in the evaluation of the order of the transition as well as the possibility of tuning the sample compositions towards the critical point. These results are compared to those of an independent method based on the temperature evolution of the hyperfine field obtained by ^{57}Fe Mössbauer spectrometry.

2. Materials and methods

The studied $La(Fe,Mn,Si)_{13H}$ granules (Calorivac-H) were manufactured by Vacuumschmelze GmbH & Co. using powder metallurgy as described in [26,27]. After loading the alloys with hydrogen, the granules were sieved to 500 – 800 µm for further investigation. Their nominal compositions are given in Table 1. The Mn content will be used as the sample designation in this work: Mn0.11, Mn0.28, Mn0.42 and Mn0.55. The phase constituents were studied by X-ray diffraction (XRD) using a Bruker D8 ADVANCE A25 diffractometer with Cu-Kα radiation performed at room temperature. Rietveld refinements were carried out by TOPAS 5.0 software. Mössbauer spectra were obtained using a conventional constant acceleration transmission spectrometer with a ^{57}Co(Rh) source (925 MBq activity) and an α-Fe foil as calibration sample. Mössbauer spectra of powder samples containing 5 mg Fe/cm^2 were recorded at various temperatures under vacuum using a homemade cryofurnace to follow the evolution of the hyperfine structure. The fittings of the spectra were conducted by MOSFIT software.

Table 1
Nominal compositions of the studied series.

Sample ID	Nominal Composition
Mn0.11	$La_1Fe_{11.63}Mn_{0.11}Si_{1.27}$
Mn0.28	$La_1Fe_{11.38}Mn_{0.28}Si_{1.34}$
Mn0.42	$La_1Fe_{11.21}Mn_{0.42}Si_{1.36}$
Mn0.55	$La_1Fe_{11.09}Mn_{0.55}Si_{1.36}$

Magnetization (M) vs. magnetic field (H) measurements up to 1.5 T were performed in a Vibrating Sample Magnetometer (VSM, LakeShore 7407) under isothermal conditions from 240 to 360 K. The isothermal entropy change (ΔS_{iso}) was indirectly determined, via Maxwell relation, from the isothermal magnetization measurements. The discontinuous measurement protocol [10] was used to remove the prior sample history between measurements, which prevents spurious results irrespective of the order of the thermomagnetic phase transition [10,28].

The magnetic field dependence of ΔS_{iso} adopts a power law expression in the form $\Delta S_{iso} \propto H^n$, [29] where its exponent n depends on both magnetic field and temperature (T). It can be calculated as follows:

$$n(T, H) = \mathrm{d}\ln|\Delta S_{iso}|/\mathrm{d}\ln|H|. \quad (1)$$

Based on the analysis of this magnitude, we are able to distinguish the order of phase transitions undergone by magnetic materials as explained before [22,25].

An additional figure of merit of the magnetocaloric materials used in this work is the temperature averaged entropy change, TEC, which avoids the artificially large refrigerant capacity of shallow responses [30]. It relates to the maximum average of the ΔS_{iso} over a temperature span (δT) and can be calculated as:

$$TEC(\delta T) = \frac{1}{\delta T} max\left(\int_{T-0.5\delta T}^{T+0.5\delta T} \Delta S_{iso}(T')\mathrm{d}T'\right), \quad (2)$$

where T_{pk} is the temperature corresponding to the peak value of ΔS_{iso}.

3. Results and discussion

The amount of the desired $NaZn_{13}$-type (1:13) phase together with the crystal parameters are evaluated by XRD. Detailed description of the crystal structure as well as presented symmetries of 1:13 phase can be found in ref.[31]. Fig. 1 shows the Rietveld

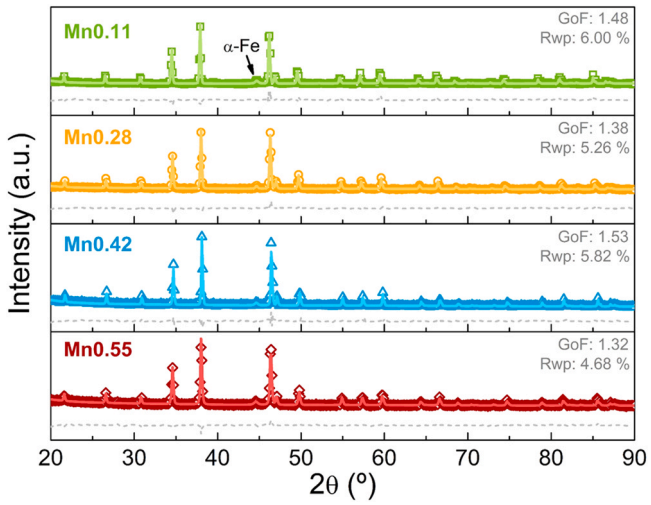

Fig. 1. Rietveld refinement of the XRD patterns collected at room temperature for the studied series.

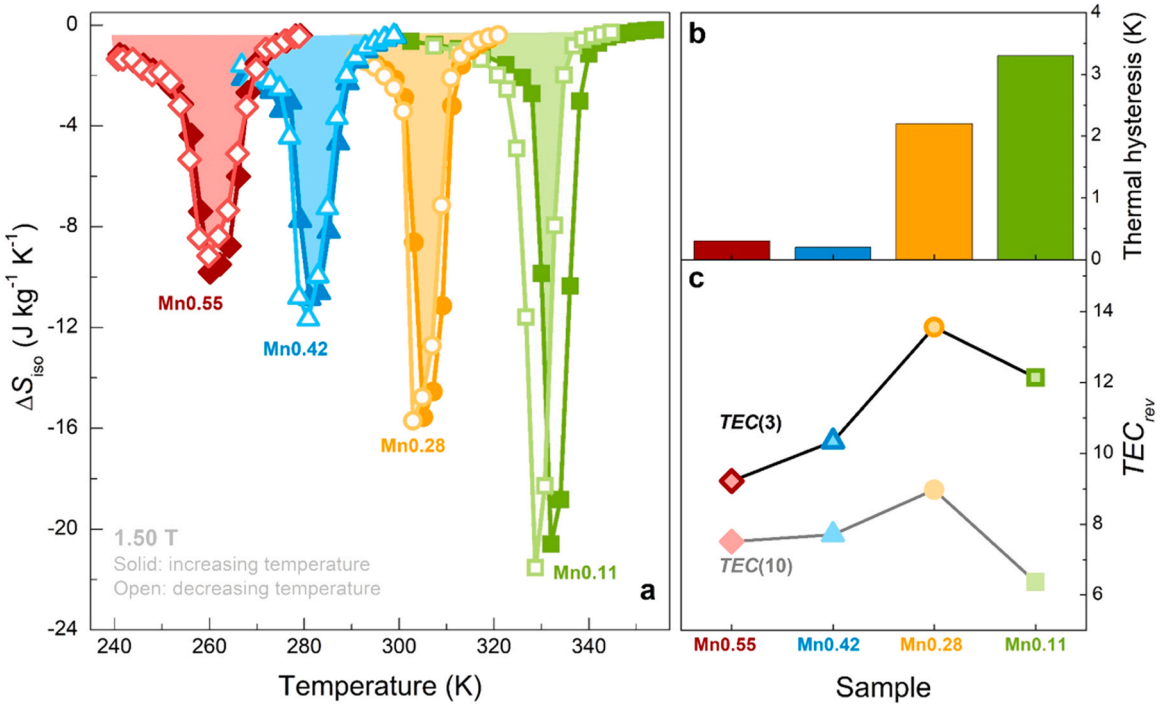

Fig. 2. (a) Isothermal entropy change, (b) thermal hysteresis and (c) reversible *TEC* response of $La(Fe,Mn,Si)_{13H}$ series for 1.5 T.

refinement of the room temperature XRD of the studied $La(Fe,Mn,Si)_{13}H$ series. R_{wp} factor close to 5% and goodness of fit (GoF) close to 1.5 are achieved for all refinements employing 1:13 and α-Fe phases, which illustrates a good fit of the results. Only minority α-Fe phase (from a minimum content of 3.4(5) to maximum content of 5.4(9) wt% in the series) in addition to the main 1:13 phase is observed, revealing the excellent quality of the samples. The lattice parameter for the 1:13 phase reduces from 11.6244(3) to 11.5541(4) Å for Mn0.11→ Mn0.55 samples.

Although this system was originally studied due to its soft magnetic character [32], it is nowadays widely investigated for its excellent magnetocaloric properties [33]. Regarding the magnetocaloric performance of the series, Fig. 2 **(a)** shows the temperature dependence of the isothermal entropy change for 1.5 T, where the samples are observed to exhibit direct MCE. Their peak values of isothermal entropy change ($|\Delta S_{iso}^{pk}|$) decrease almost linearly from 21.53 to 9.8 J $kg^{-1}K^{-1}$ with increasing Mn content. These magnitudes are comparable to those recently reported for $La(Fe,Si)_{13}$ family [33–41]. In addition, it can be

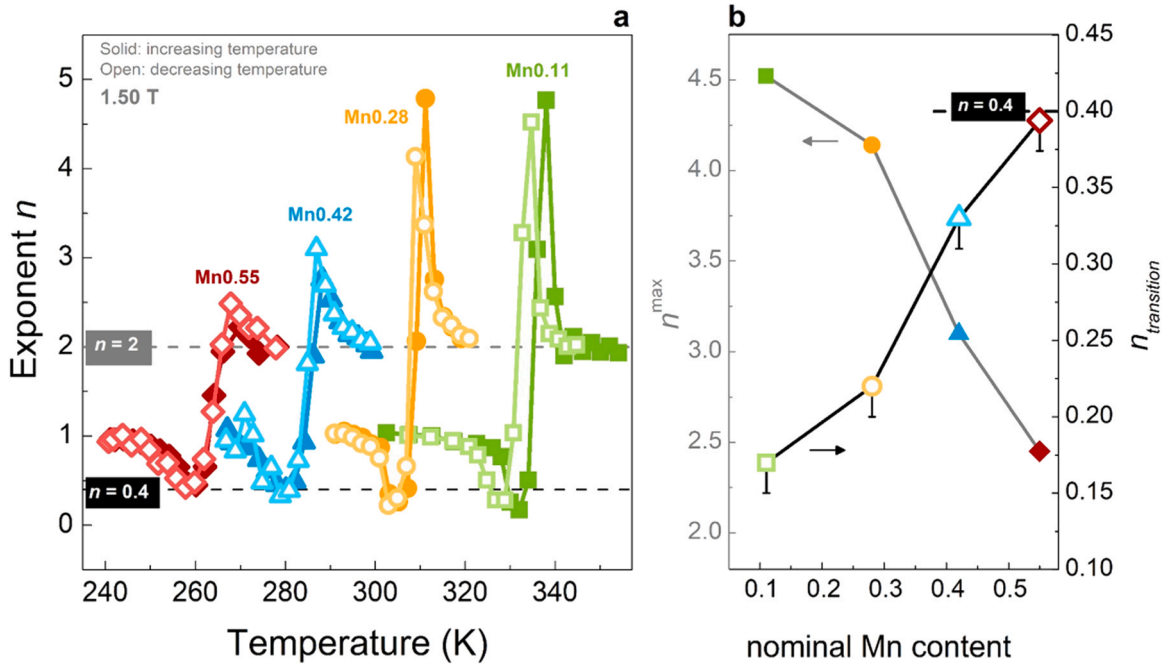

Fig. 3. First-order phase transition evidence by the (a) overshoot $n > 2$ criterion and (b) $n_{transition}$ smaller than the critical point criterion ($n_{transition} = 0.4$; represented by the black dash line).

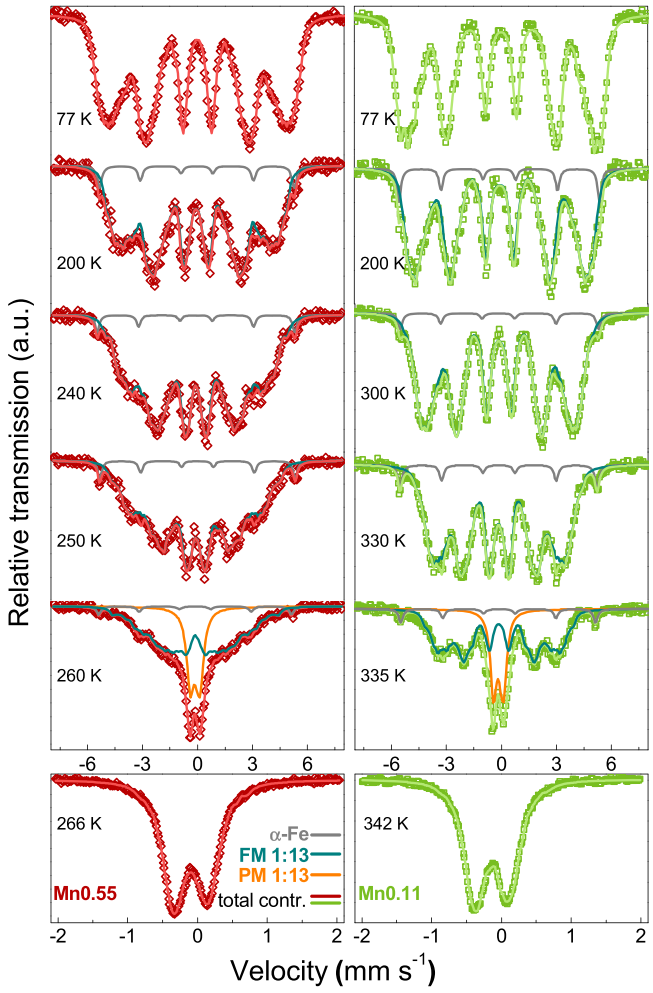

Fig. 4. Mössbauer data of Mn0.55 and Mn0.11 samples at various temperatures selected according to their phase transition temperatures (FM = ferromagnetic, PM = paramagnetic).

noticed that the shapes of the MCE curves for Mn0.42 and Mn0.55 samples are more gradual than those of Mn0.11 and Mn0.28. For the measurements made in heating protocol, the data are presented with solid symbols while those in cooling protocol are with open symbols. The shaded regions between these heating and cooling MCE curves correspond to the cyclic/reversible magnetocaloric responses that can be obtained. In addition, the thermal hysteresis between heating and cooling ΔS_{iso} curves for 1.5 T are shown in Fig. 2 **(b)**. A decrease in thermal hysteresis is observed with increasing Mn content. For Mn0.42 and Mn0.55 samples, their hysteresis is rather low even for lower magnetic fields (2.2 and 2.3 K respectively). Such low values might even be due to the thermal inertia of the experiments. These observations, when using conventional methods to identify the order of phase transition, could lead to interpret that Mn0.42 and Mn0.55 resemble SOPT character, which will be further analyzed by the exponent n analysis and Mössbauer spectrometry. We can also analyze the cyclic response, with Fig. 2 **(c)** showing the reversible contribution to $TEC(3)$ and $TEC(10)$ magnitudes based on the results for 1.5 T. A non-monotonic trend is observed for both 3 and 10 K temperature span, which are specifically selected for covering the realistic performance range of future devices [30], reaching a maximum for Mn0.28 with very attractive values. The compositional range to achieve better reversible performance is relatively narrow, making further optimization very challenging. This is because there is a link between the reduction of hysteresis (which increases TEC_{rev}) and the decrease of the maximum $|\Delta S_{iso}^{pk}|$ (which has deleterious effects on TEC_{rev}).

The magnetic field dependence exponent n has been recently reported to distinguish FOPT with a characteristic fingerprint. It has been found applicable to several families of magnetocaloric materials [14,19,20,22,42–45] even in complex samples [46]. In addition, it can be used to reveal the coexistence of overlapping thermomagnetic phase transitions, either being FOPT+SOPT [47,48] or a combination of SOPTs [49,50]. While for ferromagnetic samples n remains positive, a recent work on the n analysis to evaluate for antiferromagnetic to ferromagnetic magnetoelastic transitions reports that n values are negative at temperatures close to such transitions [51]. For the studied $La(Fe,Mn,Si)_{13}H$ series, their exponent n values, as shown in Fig. 3 **(a)**, begin at the magnitude of 1 at low temperature (due to their ferromagnetic state). Exponent n values are then observed to decrease to a minimum and then abruptly increase, showing an overshoot of $n > 2$ near their transition temperatures, indicating the FOPT character of all samples. Eventually, the n values decrease towards $n = 2$ (marked as gray dash line) due to the paramagnetic state. The maximum and minimum n values near the transition temperatures plotted as a function of Mn dependence in Fig. 3 **(b)** further illustrate that the FOPT overshoot decreases with higher Mn content. This indicates that the FOPT character decreases with Mn additions, which can be ascribed to the observed decrease in the sharpness of the MCE curve shapes for higher Mn content in Fig. 2 **(a)**. A further investigation of n values at the zero field transition temperatures, $n_{transition}$, as shown in Fig. 3 **(b)** reveals that they are all below the critical point criterion, $n_{transition} = 0.4$ (marked as black dash lines). In addition, in the absence of α-Fe contribution, the $n_{transition}$ values will be lowered as indicated by the error margins in panel b. This further indicates that the studied compositions are within the FOPT region of $La(Fe,Mn,Si)_{13H}$. The observed increase in $n_{transition}$ with Mn additions indicates that the FOPT character decreases with Mn content, which agrees to the maximum n values obtained from the FOPT overshoot (left y-axis of Fig. 3 **(b)** represented by solid symbols connected by a gray line). It must be highlighted that the $n_{transition}$ of Mn0.55 sample is relatively near to the critical point (black dash line), whereby this proximity explains the negligible hysteresis observed in Fig. 2 **(a)**. Moreover, it is possible to estimate the critical composition by extrapolating the $n_{transition}$ values up to 0.4, which corresponds to a Mn content of 0.58(2).

The phase transition is further studied by ^{57}Fe Mössbauer spectrometry, for which the results of the ends of the series, i.e., Mn0.11 and Mn0.55, are shown in Fig. 4 **(a)**. At 77 K, in the ferromagnetic state, the hyperfine structures result from a magnetic sextet with broadened lines well described by a discrete number of magnetic components or a continuous hyperfine field distribution. At high temperatures, in the paramagnetic state, the spectra show an asymmetric quadrupole doublet that can be well described by, either at least three quadrupole components, or a discrete distribution of quadrupolar splitting linearly correlated to that of isomer shift. The refined values of the hyperfine parameters for both ferromagnetic and paramagnetic states are listed in Table 2. At intermediate temperatures, two main phenomena are observed. (i) Some lines emerge to form a magnetic sextet clearly attributed to the α-Fe phase (gray line), in agreement with XRD and Rietveld refinement results (Fig. 1). In addition, (ii) below the estimated temperature of the complete magnetic order, we observe the superposition of a magnetic sextet (dark cyan line; magnetic) with broadened lines and a quadrupolar doublet (orange line; paramagnetic) growing in the center of the spectrum, both attributed to Fe species in the 1:13 phase. At this stage, it is difficult to accurately distinguish between the two components (the lower boundary value of the hyperfine field competing with the higher boundary value of the quadrupolar splitting), but it is important to note that the physical characteristics of the hyperfine parameters of the 1:13 phase result from average values that are independent of the fitting model.

Table 2
Refined values of the hyperfine parameters estimated from the Mössbauer spectra: isomer shift (IS), quadrupolar shift (2ε), hyperfine field (B_{HF}) and quadrupolar splitting (QS).

Sample	FM state			Transition temperature ± 1 (K)	PM state	
	< IS > ± 0.01 (mm/s)	< 2ε > ± 0.01 (mm/s)	< B_{hf} > ± 0.5 (T)		< IS > ± 0.01 (mm/s)	< QS > ± 0.01 (mm/s)
Mn0.11	0.15	0.00	31.2	340	-0.03	0.45
Mn0.28	0.14	0.00	29.3	312	0.00	0.50
Mn0.42	0.15	0.00	27.7	287	0.02	0.51
Mn0.55	0.15	0.01	27.5	265	0.02	0.51

FM state is taken at 77 K while PM at 1 K above the transition.

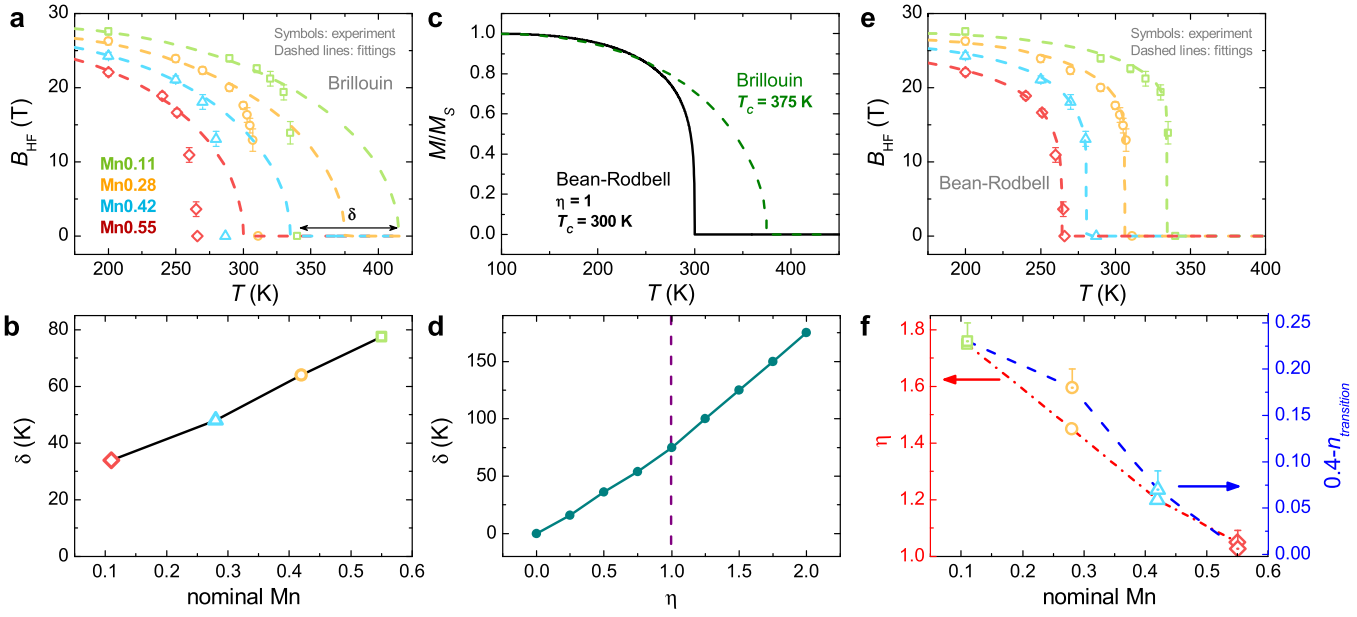

Fig. 5. (a) Hyperfine field fitted to the Brillouin function and (b) temperature difference, δ, between the transition temperature obtained from the fitting versus experimental results. (c) Reduced magnetization for the critical composition in the Bean-Rodbell model ($\eta = 1$) fitted to the Brillouin function and (d) δ as a function of the order parameter η in the model. (e) Hyperfine field fitted to the Bean-Rodbell model and (f) obtained order parameter η (left axis) compared to the 0.4- $n_{transition}$ from the previous results from exponent n criterion (right axis).

The temperature dependence of the average hyperfine field (< B_{HF} >) of the 1:13 phase for zero applied field is employed to further corroborate the order of the transitions. One widely employed method to identify FOPT from the Mössbauer experiments is to fit the experimental < B_{HF} > in the ferromagnetic range using a Brillouin function, where the separation between the experimental transition temperature and that obtained from the Brillouin fitting (δ parameter) indicates the FOPT character [52–54]. Fig. 5 **(a)** shows the different Brillouin fits (with ½ spin due to the itinerant character of the 1:13 phase [53,55]) while Fig. 5 **(b)** presents the obtained δ values. These results apparently suggest that the FOPT character could be evidenced as $\delta > 0$ for all the series although it decreases with Mn additions. Even so, the δ value for Mn0.55 sample is still far from zero, despite being close to the critical composition as shown in the analysis based on exponent n. To evaluate this discrepancy, we employ the Bean-Rodbell model [56]. This model, like the Brillouin function, is based on mean-field assumptions but it includes a magneto-volume coupling term that allows it to reproduce either SOPT or FOPT by changing the order parameter η (where < 1 indicates SOPT, > 1 for FOPT and =1 for the critical point). It has been shown that Bean-Rodbell model accurately reproduces the characteristics of the $La(Fe,Si)_{13}$ system [55,57–59]. As an example, Fig. 5 **(c)** shows how the Brillouin fitting for the critical point ($\eta = 1$) can lead to δ values that clearly differ from 0, in agreement with the results of Fig. 5 **(b)**, with δ values different from 0 even for samples close to the critical point. By performing a systematic Brillouin fitting of simulated data for different η values, Fig. 5 **(d)** shows δ as a function of the order parameter, η, where $\delta = 0$ is only reached for the $\eta = 0$ case, i.e., for SOPT without magneto-volume effect. This shows that the Brillouin fits cannot clearly differentiate between FOPT and SOPT as there is no evident threshold value for the critical composition. However, Brillouin fits can indicate a reduction in the magneto-volume coupling. Thus, we have alternatively employed the Bean-Rodbell model to determine the order of the transition from the < B_{HF} > data, as shown in Fig. 5 **(e)** (with ½ spin and a compressibility value of $8.6 \cdot 10^{-12}$ Pa^{-1} [57,58]). The obtained order parameter, η, as a function of Mn content is shown in the left y-axis of Fig. 5 **(f)** while the right y-axis presents 0.4-$n_{transition}$, which is the proximity to critical composition based on the n criteria. It is now observed that the Mössbauer fits and magnetocaloric-based n criteria show excellent agreement, indicating the FOPT character of the studied series and the reduction of the magneto-volume coupling with increasing Mn content. We can highlight that both methods clearly evidence the proximity of the critical composition for the Mn0.55 sample. It should be noted that while this Mössbauer fit makes it possible to recognize the first-order character, it is not as straightforward as the exponent n criterion, considering that obtaining exponent n does not require any fitting procedure.

4. Conclusions

New methods based on the analysis of the field dependence of the magnetocaloric effect have been employed to unambiguously determine the order of phase transition in a series of low hysteretic

high-performance La(Fe,Mn,Si)$_{13}$H materials. Their excellent cyclic performance arises from their proximity to the critical composition where FOPT crossovers to SOPT, making it challenging for conventional methods to distinguish the character of the transition. The field dependence exponent n shows the FOPT criterion of $n > 2$ overshoot near the transition temperatures for all the samples, including the one with lowest hysteresis. In addition, the analysis determines a reduction of the FOPT character as Mn content increases. Using the $n_{\text{transition}} = 0.4$ criterion for the determination of the critical composition of FOPT→ SOPT, the corresponding Mn content of this series is calculated to be 0.58(2). Furthermore, temperature dependent Mössbauer spectrometry is used as a complementary technique to evaluate for the order of the phase transition, where the FOPT character of the series is further confirmed by examining the temperature evolution of the hyperfine field. As it is a zero-field technique, the agreement between the identification of the order of the phase transition using Mössbauer spectrometry and the n-exponent criterion is a significant confirmation of the validity of the latter methodology. It turns out, however, that the exponent n analysis and criterion provide a more straightforward approach to evaluating FOPT since they uniquely identify the critical composition and its proximity without requiring complicated fitting models, in contrast to the Mössbauer results, which should be analyzed in combination with fits to a Bean-Rodbell model, rather than to the more usual Brillouin function.

CRediT authorship contribution statement

Luis M. Moreno-Ramírez: Formal analysis, Investigation, Methodology, Writing – original draft. **Jia Yan Law:** Formal analysis, Investigation, Methodology, Visualization, Writing – original draft. **Josefa M. Borrego:** Formal analysis, Writing – review & editing. **Alexander Barcza:** Resources, Writing – review & editing. **Jean-Marc Greneche:** Investigation, Formal analysis, Writing – review & editing. **Victorino Franco:** Conceptualization, Formal analysis, Methodology, Supervision, Validation, Writing – review & editing, Funding acquisition.

Data Availability

Data will be made available on request.

Declaration of Competing Interest

The authors declare that they have no known competing financial interests or personal relationships that could have appeared to influence the work reported in this paper.

Acknowledgements

Work supported by Grant funded by PID2019-105720RB-I00/AEI/10.13039/501100011033, Consejería de Economía, Conocimiento, Empresas y Universidad de la Junta de Andalucía (grant P18-RT-746), and Air Force Office of Scientific Research (FA8655-21-1-7044). JYL acknowledges EMERGIA Fellowship from Junta de Andalucía (EMC21_00418).

References

[1] EPA, Climate Change Indicators: Residential Energy Use, 2021. ⟨https://www.epa.gov/climate-indicators/climate-change-indicators-residential-energy-use⟩.
[2] IEA, The Future of Cooling, 2018. ⟨https://www.iea.org/reports/the-future-of-cooling⟩.
[3] A. Kitanovski, J. Tušek, U. Tomc, U. Plaznik, M. Ožbolt, A. Poredoš, Magnetocaloric energy conversion: from theory to applications, Springer, Cham, 2015.
[4] V. Franco, J.S. Blazquez, J.J. Ipus, J.Y. Law, L.M. Moreno-Ramirez, A. Conde, Magnetocaloric effect: from materials research to refrigeration devices, Prog. Mater. Sci. 93 (2018) 112–232.
[5] A. Kitanovski, Energy applications of magnetocaloric materials, Adv. Energy Mater. 10 (2020) 1903741.
[6] O. Gutfleisch, V. Franco, Preface to the viewpoint set on: magnetic materials for energy, Scr. Mater. 67 (2012) 521–523.
[7] J.Y. Law, V. Franco, Pushing the limits of magnetocaloric high-entropy alloys, APL Mater. 9 (2021) 080702.
[8] J.Y. Law, V. Franco, Review on magnetocaloric high-entropy alloys: design and analysis methods, J. Mater. Res 38 (2023) 37–51.
[9] J.Y. Law, L.M. Moreno-Ramirez, Á. Díaz-García, V. Franco, Current perspective in magnetocaloric materials research, J Appl Phys 133 (2023) 040903, https://doi.org/10.1063/5.0130035
[10] V. Franco, Á. Díaz-García, L.M. Moreno-Ramirez, J.Y. Law, Magnetocaloric Characterization for the Study of Phase Transitions, in: K.G. Sandeman, O. Gutfleisch (Eds.), Magnetic cooling: from fundamentals to high efficiency refrigeration Wiley, In Press, 2023.
[11] V.K. Pecharsky, J.K.A. Gschneidner, Giant magnetocaloric effect in $Gd_5(Si_2Ge_2)$, Phys. Rev. Lett. 78 (1997) 4494–4497.
[12] J. Liu, T. Gottschall, K.P. Skokov, J.D. Moore, O. Gutfleisch, Giant magnetocaloric effect driven by structural transitions, Nat. Mater. 11 (2012) 620–626.
[13] A.N. Khan, L.M. Moreno-Ramírez, Á. Díaz-García, J.Y. Law, V. Franco, All-d-metal Ni(Co)-Mn(X)-Ti (X = Fe or Cr) Heusler alloys: Enhanced magnetocaloric effect for moderate magnetic fields, J. Alloy Compd. 931 (2023) 167559.
[14] Á. Díaz-García, J. Revuelta, L.M. Moreno-Ramírez, J.Y. Law, C. Mayer, V. Franco, Additive manufacturing of magnetocaloric (La,Ce)(Fe,Mn,Si)$_{13}$–H particles via polymer-based composite filaments, Compos. Commun. 35 (2022) 101352.
[15] J.Y. Law, L.M. Moreno-Ramirez, Á. Díaz-García, V. Franco, Current perspective in magnetocaloric materials research, J. Appl. Phys. 133 (2023) 040903.
[16] L.M. Moreno-Ramírez, J.Y. Law, Á. Díaz-García, V. Franco, Advanced magnetocaloric materials, Encyclopedia of Materials: Electronics, Elsevier, 2023, https://doi.org/10.1016/B978-0-12-819728-8.00068-1
[17] K. Morrison, L.F. Cohen, Overview of the characteristic features of the magnetic phase transition with regards to the magnetocaloric effect: the hidden relationship between hysteresis and latent heat, Metall. Mater. Trans. E 1 (2014) 153–159.
[18] O. Gutfleisch, T. Gottschall, M. Fries, D. Benke, I. Radulov, K.P. Skokov, H. Wende, M. Gruner, M. Acet, P. Entel, M. Farle, Mastering hysteresis in magnetocaloric materials, Philos. Trans. R. Soc. A-Math. Phys. Eng. Sci. 374 (2016) 20150308.
[19] L.M. Moreno-Ramírez, C. Romero-Muñiz, J.Y. Law, V. Franco, A. Conde, I.A. Radulov, F. Maccari, K.P. Skokov, O. Gutfleisch, The role of Ni in modifying the order of the phase transition of La(Fe,Ni,Si)$_{13}$, Acta Mater. 160 (2018) 137–146.
[20] L.M. Moreno-Ramírez, C. Romero-Muñiz, J.Y. Law, V. Franco, A. Conde, I.A. Radulov, F. Maccari, K.P. Skokov, O. Gutfleisch, Tunable first order transition in La(Fe,Cr,Si)$_{13}$ compounds: retaining magnetocaloric response despite a magnetic moment reduction, Acta Mater. 175 (2019) 406–414.
[21] L.M. Moreno-Ramirez, V. Franco, Reversibility of the magnetocaloric effect in the Bean-Rodbell model, Magnetochemistry 7 (2021).
[22] J.Y. Law, V. Franco, L.M. Moreno-Ramirez, A. Conde, D.Y. Karpenkov, I. Radulov, K.P. Skokov, O. Gutfleisch, A quantitative criterion for determining the order of magnetic phase transitions using the magnetocaloric effect, Nat. Commun. 9 (2018) 2680.
[23] S. Bustingorry, F. Pomiro, G. Aurelio, J. Curiale, Second-order magnetic critical points at finite magnetic fields: revisiting Arrott plots, Phys. Rev. B 93 (2016) 224429.
[24] C.M. Bonilla, J. Herrero-Albillos, F. Bartolome, L.M. Garcia, M. Parra-Borderias, V. Franco, Universal behavior for magnetic entropy change in magnetocaloric materials: an analysis on the nature of phase transitions, Phys. Rev. B 81 (2010) 224424.
[25] V. Franco, J.Y. Law, A. Conde, V. Brabander, D. Karpenkov, I. Radulov, K. Skokov, O. Gutfleisch, Predicting the tricritical point composition of a series of LaFeSi magnetocaloric alloys via universal scaling, J. Phys. D: Appl. Phys. 50 (2017) 414004.
[26] A. Barcza, M. Katter, V. Zellmann, S. Russek, S. Jacobs, C. Zimm, Stability and magnetocaloric properties of sintered La(Fe, Mn, Si)$_{13}$H$_z$ Alloys, Ieee Trans. Magn. 47 (2011) 3391–3394.
[27] M. Katter, V. Zellmann, G.W. Reppel, K. Uestuener, Magnetocaloric properties of La(Fe, Co, Si)$_{13}$ bulk material prepared by powder metallurgy, Ieee Trans. Magn. 44 (2008) 3044–3047.
[28] B. Kaeswurm, V. Franco, K.P. Skokov, O. Gutfleisch, Assessment of the magnetocaloric effect in La,Pr(Fe,Si) under cycling, J. Magn. Magn. Mater. 406 (2016) 259–265.
[29] V. Franco, A. Conde, Scaling laws for the magnetocaloric effect in second order phase transitions: From physics to applications for the characterization of materials, Int. J. Refrig. 33 (2010) 465–473.
[30] L.D. Griffith, Y. Mudryk, J. Slaughter, V.K. Pecharsky, Material-based figure of merit for caloric materials, J. Appl. Phys. 123 (2018) 034902.
[31] M. DeGraef, M.E. McHenry, Structure of Materials, Cambridge University Press, 2007.
[32] M.Q. Huang, W.E. Wallace, R.T. Obermyer, S. Simizu, M. McHenry, S.G. Sankar, Magnetic characteristics of RCo13−xSix alloys (R=La, Pr, Nd, Gd, and Dy), J. Appl. Phys. 79 (1996) 5949–5951.
[33] A. Fujita, S. Fujieda, Y. Hasegawa, K. Fukamichi, Itinerant-electron metamagnetic transition and large magnetocaloric effects in La(Fe$_x$Si$_{1-x}$)$_{13}$ compounds and their hydrides, Phys. Rev. B 67 (2003) 104416.
[34] K. Xu, Y. Hu, H. Song, S. Huang, J. Zhang, J. Fang, X. Hu, X. Hou, Modification of magneto-caloric effect in spherical La-Fe-Co-Si compounds particles by hydrogen permeation, J. Alloy Compd. 918 (2022) 165568.

[35] R. Zhang, X. Zhang, M. Qian, C.R.H. Bahl, Optimization of microstructure and magnetocaloric effect by heat treatment process in $LaFe_{11.7}Si_{1.3}$ microwire, J. Alloy Compd. 890 (2022) 161845.
[36] K. Imaizumi, A. Fujita, A. Suzuki, M. Kobashi, K. Ozaki, Improvement of magnetocaloric effect in $La(Fe_xSi_{1-x})_{13}$ by dealing with inhibitory microstructures at high Fe concentration, Acta Mater. 227 (2022) 117726.
[37] Y. Liu, X. Fu, Q. Yu, M. Zhang, J. Liu, Significant reduction of phase-transition hysteresis for magnetocaloric $(La_{1-x}Ce)_2Fe11Si_2H$ alloys by microstructural manipulation, Acta Mater. 207 (2021).
[38] X. Lu, Y. Zhang, F. Wang, M. Zhang, J. Liu, On the microstructural evolution and accelerated magnetocaloric phase formation in La-Fe-Si alloys by hot forging deformation, Acta Mater. (2021).
[39] H. Zhou, Y. Long, S. Miraglia, F. Porcher, H. Zhang, Age stability of $La(Fe,Si)_{13}$ hydrides with giant magnetocaloric effects, Rare Met. 41 (2021) 992–1001.
[40] T. Gottschall, K.P. Skokov, M. Fries, A. Taubel, I. Radulov, F. Scheibel, D. Benke, S. Riegg, O. Gutfleisch, Making a cool choice: the materials library of magnetic refrigeration, Adv. Energy Mater. 9 (2019) 1901322.
[41] M. Krautz, K. Skokov, T. Gottschall, C.S. Teixeira, A. Waske, J. Liu, L. Schultz, O. Gutfleisch, Systematic investigation of Mn substituted $La(Fe,Si)_{13}$ alloys and their hydrides for room-temperature magnetocaloric application, J. Alloy Compd. 598 (2014) 27–32.
[42] J.Y. Law, Á. Díaz-García, L.M. Moreno-Ramírez, V. Franco, Increased magnetocaloric response of FeMnNiGeSi high-entropy alloys, Acta Mater. 212 (2021) 116931.
[43] J.Y. Law, L.M. Moreno-Ramírez, Á. Díaz-García, A. Martín-Cid, S. Kobayashi, S. Kawaguchi, T. Nakamura, V. Franco, MnFeNiGeSi high-entropy alloy with large magnetocaloric effect, J. Alloy Compd. 855 (2021) 157424.
[44] R. M'Nassri, M.M. Nofal, P. de Rango, N. Chniba-Boudjada, Magnetic entropy table-like shape and enhancement of refrigerant capacity in $La_{1.4}Ca_{1.6}Mn_2O_7$-$La_{1.3}Eu_{0.1}Ca_{1.6}Mn_2O_7$ composite, RSC Adv. 9 (2019) 14916–14927.
[45] W. Liu, F. Scheibel, T. Gottschall, E. Bykov, I. Dirba, K. Skokov, O. Gutfleisch, Large magnetic entropy change in Nd_2In near the boiling temperature of natural gas, Appl. Phys. Lett. 119 (2021).
[46] J.Y. Law, V. Franco, A. Conde, S. Skinner, S. Pramana, Modification of the order of the magnetic phase transition in cobaltites without changing their crystal space group, J. Alloy Compd. 777 (2019) 1080–1086.
[47] J.Y. Law, Á. Díaz-García, L.M. Moreno-Ramírez, V. Franco, A. Conde, A.K. Giri, How concurrent thermomagnetic transitions can affect magnetocaloric effect: the $Ni_{49-x}Mn_{36+x}In_{15}$ Heusler alloy case, Acta Mater. 166 (2019) 459–465.
[48] Á. Díaz-García, J.Y. Law, L.M. Moreno-Ramírez, A.K. Giri, V. Franco, Deconvolution of overlapping first and second order phase transitions in a NiMnIn Heusler alloy using the scaling laws of the magnetocaloric effect, J. Alloy Compd. 871 (2021) 159621.
[49] P. Gębara, Á. Díaz-García, J.Y. Law, V. Franco, Magnetocaloric response of binary Gd-Pd and ternary Gd-(Mn,Pd) alloys, J. Magn. Magn. Mater. 500 (2020) 166175.
[50] Á. Díaz-García, J.Y. Law, P. Gębara, V. Franco, Phase deconvolution of multiphasic materials by the universal scaling of the magnetocaloric effect, Jom 72 (2020) 2845–2852.
[51] L.M. Moreno-Ramírez, J.Y. Law, S.S. Pramana, A.K. Giri, V. Franco, Analysis of the magnetic field dependence of the isothermal entropy change of inverse magnetocaloric materials, Results Phys. 22 (2021) 103933.
[52] X.B. Liu, D.H. Ryan, Z. Altounian, The order of magnetic phase transition in $La(Fe_{1-x}Co_x)_{11.4}Si_{1.6}$ compounds, J. Magn. Magn. Mater. 270 (2004) 305–311.
[53] G.J. Wang, F. Wang, N.L. Di, B.G. Shen, Z.H. Cheng, Hyperfine interactions and band structures of $LaFe_{13-x}Si_x$ intermetallic compounds with large magnetic entropy changes, J. Magn. Magn. Mater. 303 (2006) 84–91.
[54] D.H. Ryan, N. Mas, R.A. Susilo, J.M. Cadogan, R. Flacau, Determination of the magnetic structure of $Gd_2Fe_2Si_2C$ by Mossbauer spectroscopy and neutron diffraction, J. Phys. Condens. Matter.: Inst. Phys. J. 27 (2015) 146005.
[55] D.Y. Karpenkov, A.Y. Karpenkov, K.P. Skokov, I.A. Radulov, M. Zheleznyi, T. Faske, O. Gutfleisch, Pressure Dependence of magnetic properties in $La(Fe,Si)_{13}$ multistimulus responsiveness of caloric effects by modeling and experiment, Phys. Rev. Appl. (2020) 034014.
[56] C. Bean, D. Rodbell, Magnetic disorder as a first-order phase transformation, Phys. Rev. 126 (1962) 104–115.
[57] L.M. Moreno-Ramirez, J.S. Blazquez, I.A. Radulov, K.P. Skokov, O. Gutfleisch, V. Franco, A. Conde, Combined kinetic and Bean-Rodbell approach for describing field-induced transitions in LaFe11.6Si1.4 alloys, J. Phys. D. Appl. Phys. 54 (2021) 135003.
[58] L. Jia, J.R. Sun, H.W. Zhang, F.X. Hu, C. Dong, B.G. Shen, Magnetovolume effect in intermetallics $LaFe_{13-x}Si_x$, J. Phys. -Condens Mat. 18 (2006) 9999–10007.
[59] H.N. Bez, K.K. Nielsen, P. Norby, A. Smith, C.R.H. Bahl, Magneto-elastic coupling in $La(Fe, Mn, Si)_{13}Hy$ within the Bean-Rodbell model, Aip Adv. 6 (2016) 056217.